



XXVIIIth International Conference on Ultrarelativistic nucleus–nucleus Collisions  
(Quark Matter 2018)

# Quarkonium measurements in nucleus–nucleus collisions with ALICE

Pascal Dillenseger for the ALICE Collaboration

*Institut für Kernphysik - Goethe-Universität, Max-von-Laue-Straße 1, 60438 Frankfurt am Main - Germany*

## Abstract

Quarkonia, i.e. bound states of  $b\bar{b}$  and  $c\bar{c}$  quarks, are powerful observables to study the properties of nuclear matter under extreme conditions. The formation of a Quark-Gluon Plasma (QGP), which is predicted by lattice QCD calculations at high temperatures as reached at the LHC energies, has a strong influence on the production and behavior of quarkonia.

The latest ALICE results on bottomonium and charmonium production in nucleus–nucleus collisions are presented. This includes measurements of the  $\Upsilon(1S)$  and  $\Upsilon(2S)$  nuclear modification factor ( $R_{AA}$ ) at forward rapidity and the  $J/\psi$   $R_{AA}$  and  $v_2$  as a function of centrality,  $p_T$  and rapidity in Pb–Pb collisions at  $\sqrt{s_{NN}} = 5.02$  TeV. Also, first results from  $J/\psi$  measurements in Xe–Xe collisions at  $\sqrt{s_{NN}} = 5.44$  TeV are presented. Further on, the experimental results are compared to various calculations from theoretical models.

**Keywords:** Heavy-ion, ALICE, Quark-Gluon Plasma, Bottomonium, Charmonium,  $J/\psi$ , Color screening, Regeneration

## 1. Quarkonium production in nucleus–nucleus collisions

The significant enhancement of the  $J/\psi$  nuclear modification factor ( $R_{AA}$ ) at the LHC energies compared to the SPS and RHIC energies [1, 2] indicates an almost leveled competition between suppression and (re)generation of charmonium states in nucleus–nucleus collisions in the TeV regime. The  $R_{AA}$  is defined as the ratio of production yields in nucleus–nucleus collisions ( $dN_{AA}$ ) and pp collisions ( $dN_{pp}$ ) scaled with number of binary nucleon-nucleon collisions ( $N_{coll}$ ):  $R_{AA} = \frac{dN_{AA}}{N_{coll} \times dN_{pp}}$ . Heavy-quark pairs ( $Q\bar{Q}$ ), i.e.  $b\bar{b}$  and  $c\bar{c}$ , are produced in initial hard processes, thus the quarkonium bound state production is subject to the full evolution of the collision. A suppression of quarkonium states in a Quark-Gluon Plasma (QGP) is expected due to the color-screening effect, which is based on a Debye screening of the color charge [3]. In competition with the color-screening effect, where initial  $Q\bar{Q}$  pairs are separated and not able to form a bound state, is the (re)combination effect. It is based on the non-zero probability that quasi-free quarks and anti-quarks move close enough in space and momentum to form a quarkonium bound state. The influence on the quarkonium production rates of this effect is strongly coupled to the  $Q\bar{Q}$  production cross-section ( $\sigma_{Q\bar{Q}}$ ) [4, 5]. Both effects are highly sensitive to the properties of the QGP and should induce diverging behavior on the differential quarkonium production, e.g. momentum distribution and elliptic flow.

In the following, the ALICE results for quarkonium measurements in nucleus–nucleus collisions presented during the Quark Matter Conference 2018 are discussed. This includes the  $J/\psi$ - $R_{AA}$  measurement in Xe–Xe collisions at  $\sqrt{s_{NN}} = 5.44$  TeV, multi-differential  $J/\psi$ -yield measurements and differential measurements of the bottomonium  $R_{AA}$  in the forward rapidity range and the elliptic flow of  $J/\psi$  at forward and mid-rapidity in Pb–Pb collisions at  $\sqrt{s_{NN}} = 5.02$  TeV.

## 2. Experimental results of quarkonium measurements in nucleus–nucleus collisions

The ALICE experiment measures charmonia and bottomonia in their leptonic decay channels. The dimuon channel is measured at forward rapidity in the range of  $2.5 < y_{lab} < 4$  with the muon spectrometer, while the dielectron channel is measured at mid-rapidity in the range of  $-0.9 < y_{lab} < 0.9$  with the central-barrel detectors. A more detailed description of the ALICE experiment can be found in [9]. The results presented in the following are based on Pb–Pb ( $A_{Pb} = 208$ ) and Xe–Xe ( $A_{Xe} = 129$ ) collisions at  $\sqrt{s_{NN}} = 5.02$  TeV and  $\sqrt{s_{NN}} = 5.44$  TeV, respectively, provided by the LHC. The ALICE experiment was capable to record integrated luminosities of  $\mathcal{L}_{int}^{Pb} \approx 225 \mu b^{-1}$  and  $\mathcal{L}_{int}^{Xe} \approx 0.34 \mu b^{-1}$  at forward rapidity and  $\mathcal{L}_{int}^{Pb} \approx 13 \mu b^{-1}$  and  $\mathcal{L}_{int}^{Xe} \approx 0.25 \mu b^{-1}$  at mid-rapidity, respectively. The large difference, especially for the Pb–Pb sample, is due the fact that at mid-rapidity minimum bias events were selected, while at forward rapidity special muon triggers were applied during data taking [2, 6].

The  $J/\psi$   $R_{AA}$  measurement in Xe–Xe collisions at  $\sqrt{s_{NN}} = 5.44$  TeV enables the comparison between lighter (Xe) and heavier (Pb) nuclei. The measurement of the  $J/\psi$   $R_{AA}$  as a function of the average number of participants ( $\langle N_{part} \rangle$ ) [10] in the forward [6] and mid-rapidity range is shown in Fig. 1 together with the  $J/\psi$   $R_{AA}$  for Pb–Pb collisions. At forward rapidity, the results for both collision systems agree with each other for similar  $\langle N_{part} \rangle$  within uncertainties. A comparison of the measurements at forward rapidity to a transport model [7, 8] is shown in Fig. 2. The model is based on the thermal rate equation and contains continuous  $J/\psi$  dissociation and regeneration in the QGP and the hadronic phase. The two collision systems as well as data and model agree well, which indicates that similar  $\sqrt{s_{NN}}$  and  $\langle N_{part} \rangle$  lead to similar relative contributions of suppression and (re)generation. However, strong conclusions are still difficult due to the uncertainties, which for the model are driven by the uncertainties on  $\sigma_{c\bar{c}}$ .

In  $J/\psi$ - $R_{AA}$  measurements as a function of rapidity in  $\sqrt{s_{NN}} = 2.76$  TeV Pb–Pb collisions, ALICE observed an opposing trend between data [11] and cold-nuclear-matter model calculations [12, 13]. These models expected an increase of  $R_{AA}$  with rapidity, while a decrease was observed in the data. The large data sample from  $\sqrt{s_{NN}} = 5.02$  TeV Pb–Pb collisions allows a multi-differential analysis of  $J/\psi$  yields as a function of rapidity, transverse momentum and centrality [14]. First preliminary results of this analysis are

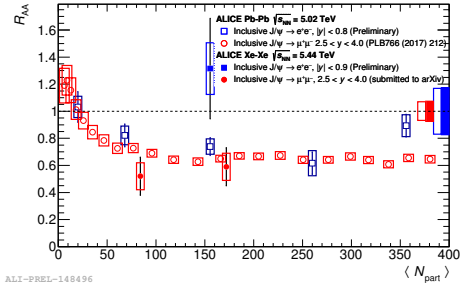


Fig. 1:  $J/\psi$   $R_{AA}$  as a function of  $\langle N_{part} \rangle$ . Red (open) circles:  $2.5 < y_{lab} < 4$ ,  $\sqrt{s_{NN}} = 5.44$  (5.02) TeV Xe–Xe (Pb–Pb) collisions [6]. Blue (open) squares:  $0.9 < |y_{lab}|$  ( $0.8 < |y_{lab}|$ ),  $\sqrt{s_{NN}} = 5.44$  (5.02) TeV Xe–Xe (Pb–Pb) collisions.

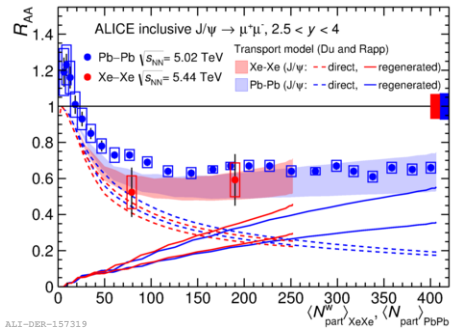


Fig. 2:  $J/\psi$   $R_{AA}$  as a function of  $\langle N_{part} \rangle$  in the range of  $2.5 < y_{lab} < 4$ . Red (blue):  $\sqrt{s_{NN}} = 5.44$  (5.02) TeV Xe–Xe (Pb–Pb) collisions [6]. Model calculations by Du and Rapp, dashed lines: direct, straight lines: regenerated, bands: incl.  $J/\psi$  [7, 8].

shown in Fig. 3a and Fig. 3b. In Fig. 3a the  $J/\psi$  yield as a function of rapidity for different  $p_T$  intervals in the 20% most central events is illustrated. The rapidity dependence is then fitted with exponential functions, the resulting slopes are depicted in Fig. 3b. The slope decreases with increasing  $p_T$  and shows only a weak dependence on centrality.

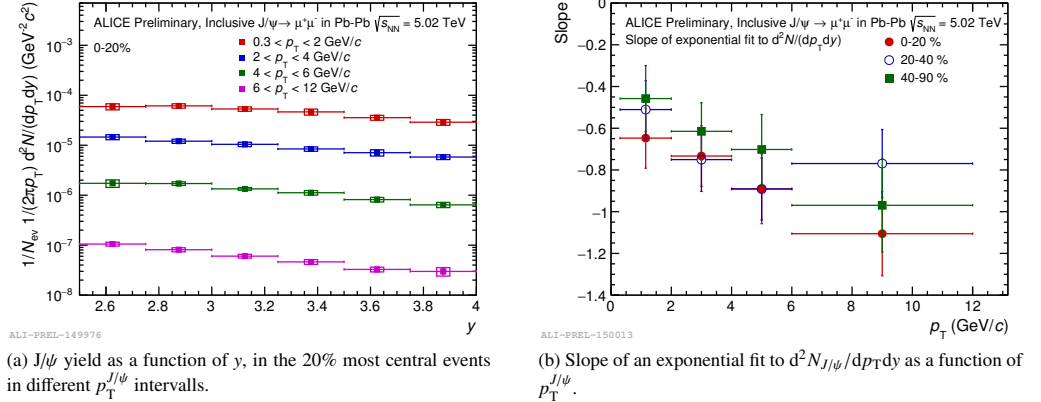


Fig. 3: Preliminary results of a multi-differential  $J/\psi$ -yield analysis in  $\sqrt{s_{NN}} = 5.02$  TeV Pb-Pb collisions.

Another way to obtain more information about the different charmonium production mechanisms is the analysis of the elliptic flow.  $J/\psi$  from (re)combined  $c\bar{c}$  quarks should inherit the charm elliptic flow, which was observed in measurements of  $D$ -mesons [15]. The results at forward rapidity show a significant positive  $J/\psi$  elliptic flow in all studied  $p_T$  bins. Within the large statistical uncertainties the measurement at mid-rapidity agrees with the one at forward rapidity [16]. A comparison to model calculations [8, 17] is shown in Fig. 4. Both models describe the data in the low- $p_T$  regime, where the elliptic flow of the models is generated by their regeneration component. At high  $p_T$  the models clearly underestimate the measured elliptic flow. The question remains open how the elliptic flow of  $J/\psi$  above  $p_T \approx 5$  GeV/c is generated.

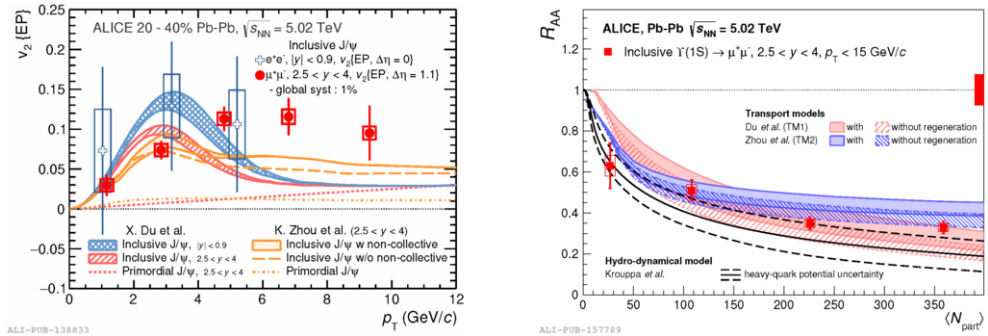


Fig. 4:  $J/\psi$  elliptic flow as a function of  $p_T$  at forward and mid-rapidity in semi-central  $\sqrt{s_{NN}} = 5.02$  TeV Pb-Pb collisions [16] compared to transport model calculations [8, 17].

Fig. 5:  $\Upsilon R_{AA}$  as a function of  $(N_{part})$  in  $\sqrt{s_{NN}} = 5.02$  TeV Pb-Pb collisions [18], compared to transport [19, 20] and hydro-dynamical [21] model calculations.

ALICE measured the  $\Upsilon(1S) R_{AA}$  as a function of  $p_T$  and  $y$  as well as the inclusive  $\Upsilon(2S) R_{AA}$  in the forward rapidity range [18]. An increase of the  $\Upsilon(1S)$  suppression towards more central events is observed, but due to the not precisely known feed-down fraction, the amount of direct  $\Upsilon(1S)$  suppression is an open question. The measurement is shown in Fig. 5 and compared with three model calculations (two transport [19, 20] and one hydro-dynamical model calculation [21]), which all agree with the data within the

uncertainties. The two transport models are shown without a regeneration component, both versions agree with the data, which indicates that a regeneration component for bottomonium should be negligible at LHC energies. The  $\Upsilon(2S)$  suppression is significantly stronger than the one of the  $\Upsilon(1S)$  visible in the ratio of the  $\Upsilon(2S)$  over  $\Upsilon(1S)$   $R_{AA}$ :  $R_{AA}^{\Upsilon(2S)}/R_{AA}^{\Upsilon(1S)} = 0.28 \pm 0.12(stat.) \pm 0.06(syst.)$ . For the  $\Upsilon(1S)$   $R_{AA}$  neither a significant dependence on  $p_T$  nor on  $y$  is observed [18].

### 3. Conclusions

Measurements of  $J/\psi$   $R_{AA}$  in Xe–Xe collisions at  $\sqrt{s_{NN}} = 5.44$  TeV and the elliptic flow and multi-differential yields of  $J/\psi$  as well as the differential (inclusive)  $\Upsilon(1S)$  ( $\Upsilon(2S)$ )  $R_{AA}$  in Pb–Pb collisions at  $\sqrt{s_{NN}} = 5.02$  TeV have been presented. The results indicate that quarkonia production at the LHC is a combination of suppression and (re)generation, strongly dependent on the  $\sigma_{Q\bar{Q}}$ . However, there are still unanswered questions, e.g. the reason for the significant  $J/\psi$  elliptic flow at higher  $p_T$  or the amount of direct  $\Upsilon(1S)$  suppression, which hopefully can be answered in the near future.

### References

- [1] PHENIX Collaboration, A. Adare, et al.,  $J/\psi$  Production vs Centrality, Transverse Momentum, and Rapidity in Au+Au Collisions at  $\sqrt{s_{NN}} = 200$  GeV, Phys. Rev. Lett. 98 (2007) 232301. arXiv:nucl-ex/0611020, doi:10.1103/PhysRevLett.98.232301.
- [2] ALICE Collaboration, J. Adam, et al.,  $J/\psi$  suppression at forward rapidity in Pb-Pb collisions at  $\sqrt{s_{NN}} = 5.02$  TeV, Phys. Lett. B766 (2017) 212–224. arXiv:1606.08197, doi:10.1016/j.physletb.2016.12.064.
- [3] T. Matsui, H. Satz,  $J/\psi$  Suppression by Quark-Gluon Plasma Formation, Phys. Lett. B178 (1986) 416–422. doi:10.1016/0370-2693(86)91404-8.
- [4] R. L. Thews, M. Schroedter, J. Rafelski, Enhanced  $J/\psi$  production in deconfined quark matter, Phys. Rev. C63 (2001) 054905. arXiv:hep-ph/0007323, doi:10.1103/PhysRevC.63.054905.
- [5] P. Braun-Munzinger, J. Stachel, (Non)thermal aspects of charmonium production and a new look at  $J/\psi$  suppression, Phys. Lett. B490 (2000) 196–202. arXiv:nucl-th/0007059, doi:10.1016/S0370-2693(00)00991-6.
- [6] ALICE Collaboration, S. Acharya, et al., Inclusive  $J/\psi$  production in Xe-Xe collisions at  $\sqrt{s_{NN}} = 5.44$  TeV (2018). arXiv:1805.04383.
- [7] X. Zhao, R. Rapp, Medium Modifications and Production of Charmonia at LHC, Nucl. Phys. A859 (2011) 114–125. arXiv:1102.2194, doi:10.1016/j.nuclphysa.2011.05.001.
- [8] X. Du, R. Rapp, Sequential Regeneration of Charmonia in Heavy-Ion Collisions, Nucl. Phys. A943 (2015) 147–158. arXiv:1504.00670, doi:10.1016/j.nuclphysa.2015.09.006.
- [9] ALICE Collaboration, K. Aamodt, et al., The ALICE experiment at the CERN LHC, JINST 3 (2008) S08002. doi:10.1088/1748-0221/3/08/S08002.
- [10] ALICE Collaboration, B. Abelev, et al., Centrality determination of Pb-Pb collisions at  $\sqrt{s_{NN}} = 2.76$  TeV with ALICE, Phys. Rev. C88 (4) (2013) 044909. arXiv:1301.4361, doi:10.1103/PhysRevC.88.044909.
- [11] ALICE Collaboration, B. B. Abelev, et al., Centrality, rapidity and transverse momentum dependence of  $J/\psi$  suppression in Pb-Pb collisions at  $\sqrt{s_{NN}}=2.76$  TeV, Phys. Lett. B734 (2014) 314–327. arXiv:1311.0214, doi:10.1016/j.physletb.2014.05.064.
- [12] R. Vogt, Cold Nuclear Matter Effects on  $J/\psi$  and  $\Upsilon$  Production at the LHC, Phys. Rev. C81 (2010) 044903. arXiv:1003.3497, doi:10.1103/PhysRevC.81.044903.
- [13] A. Rakotozafindrabe, E. Ferreira, F. Fleuret, J. Lansberg, N. Matagne, Cold Nuclear Matter effects on  $J/\psi$  production with intrinsic  $p_T$  at  $\sqrt{s_{NN}}=2.76$ TeV at the LHC, Nucl. Phys. A855 (1) (2011) 327 – 330. doi:https://doi.org/10.1016/j.nuclphysa.2011.02.071.
- [14] H. Hushnud for the ALICE Collaboration, Multi-differential study of  $J/\psi$  yield at forward rapidity in Pb-Pb collisions at  $\sqrt{s_{NN}} = 5.02$  TeV with ALICE, Poster Quark Matter Conference 2018. URL <https://indico.cern.ch/event/656452/contributions/2859764/>
- [15] ALICE Collaboration, S. Acharya, et al.,  $D$ -meson azimuthal anisotropy in Midcentral Pb–Pb collisions at  $\sqrt{s_{NN}} = 5.02$  TeV, Phys. Rev. Lett. 120 (10) (2018) 102301. arXiv:1707.01005, doi:10.1103/PhysRevLett.120.102301.
- [16] ALICE Collaboration, S. Acharya, et al.,  $J/\psi$  elliptic flow in Pb-Pb collisions at  $\sqrt{s_{NN}} = 5.02$  TeV, Phys. Rev. Lett. 119 (24) (2017) 242301. arXiv:1709.05260, doi:10.1103/PhysRevLett.119.242301.
- [17] K. Zhou, N. Xu, Z. Xu, P. Zhuang, Medium effects on charmonium production at ultrarelativistic energies available at the CERN Large Hadron Collider, Phys. Rev. C89 (5) (2014) 054911. arXiv:1401.5845, doi:10.1103/PhysRevC.89.054911.
- [18] ALICE Collaboration, S. Acharya, et al.,  $\Upsilon$  suppression at forward rapidity in Pb-Pb collisions at  $\sqrt{s_{NN}} = 5.02$  TeV (2018). arXiv:1805.04387.
- [19] X. Du, R. Rapp, M. He, Color Screening and Regeneration of Bottomonia in High-Energy Heavy-Ion Collisions, Phys. Rev. C96 (5) (2017) 054901. arXiv:1706.08670, doi:10.1103/PhysRevC.96.054901.
- [20] K. Zhou, N. Xu, P. Zhuang,  $\Upsilon$  Production in Heavy Ion Collisions at LHC, Nucl. Phys. A931 (2014) 654–658. arXiv:1408.3900, doi:10.1016/j.nuclphysa.2014.08.104.
- [21] B. Krouppa, A. Rothkopf, M. Strickland, Bottomonium suppression using a lattice QCD vetted potential, Phys. Rev. D97 (1) (2018) 016017. arXiv:1710.02319, doi:10.1103/PhysRevD.97.016017.